Article

High Performance Polymers

High Performance Polymers
24(4) 319–330

DOI: 10.1177/0954008312440470
hip.sagepub.com

Polyazomethine with vinylene and phenantridine moieties in the main chain: Synthesis, characterization, opto(electrical) properties and theoretical calculations

Agnieszka Iwan[1], Jeconias Rocha Guimarães[2], Maria Cristina dos Santos[2], Ewa Schab-Balcerzak[3], Michal Krompiec[3], Marcin Palewicz[1] and Andrzej Sikora[1]

Abstract

The opto(electrical) properties and theoretical calculations of polyazomethine with vinylene and phenantridine moieties in the main chain were investigated in the present study. 2,5-Bis(hexyloxy)-1,4-bis[(2,5-bis(hexyloxy)-4-formyl-phenylene-vinylene]benzene was polymerized in solution with 3,8-diamino-6-phenylphenanthridine (PAZ-PV-Ph). The temperatures of 5% weight loss ($T_{5\%}$) of the polyazomethine was observed at 356 °C in nitrogen. Electrochemical properties of thin film of the polymer were studied by differential pulse voltammetry. The HOMO level of the PAZ-PV-Ph was at −4.97 eV. The energy band gap (E_g) was detected of approximately ∼1.9 eV. Energy band gap (E_{gopt}) was additionally calculated from absorption spectrum and absorption coefficient α. The absorption UV-vis spectra of polyazomethine recorded in solution showed a blue shift in comparison with the solid state. HOMO-LUMO levels and E_g were additionally calculated theoretically by density functional theory and molecular simulations of PAZ-PV-Ph are presented. Current density–voltage (*J–U*) measurements were performed on ITO/PAZ-PV-Ph/Al, ITO/TiO2/PAZ-PV-Ph/Al and ITO/PEDOT/PAZ-PV-Ph:TiO2/Al devices in the dark and during irradiation with light (under illumination of 1000 W m^{-2}). The polymer was tested using AFM technique and roughness (R_a, R_{ms}) along with skew and kurtosis are presented.

Keywords

polyazomethines, current density–voltage characteristics, HOMO-LUMO, theoretical calculations

Introduction

It is well known that polyazomethines are thermostable and π-conjugated polymers and are interesting candidates for opto(electronic) applications.[1–9] However, many of these studies concern the syntheses and study of their photoluminescence properties. Among different structures of synthesized polyazomethines, polymers with vinylene moieties have not been widely investigated, the only example being the present authors' previously study.[10,11] The introduction of -CH=CH- bonds to a polyazomethine may improve its opto(electrical) properties, especially by the fact that polyazomethines are isoelectronic with poly(*p*-phenylene vinylene) (PPV).[12] On the other hand, polyazomethines based on 3,8-diamino-6-phenylphenanthridine (DAPP) have also been seldom studied.[13,14] The present authors' former works describe photoluminescence and the structural properties of polyketimines synthesized via polycondensation of various diketones with 3,8-diamino-6-phenylphenanthridine.[13,14] The emission spectra of polymers obtained from 3,8-diamino-6-phenylphenanthridine and *trans*-1,2-dibenzoylethylene, *p*-dibenzoylbenzene and dibenzyl showed maximum in the range 510–520 nm. The

[1] Electrotechnical Institute, Division of Electrotechnology and Materials Science, Wroclaw, Poland
[2] Instituto de Física, Universidade de São Paulo, São Paulo, SP, Brazil
[3] Institute of Chemistry, University of Silesia, Katowice, Poland

Corresponding author:
Agnieszka Iwan, Electrotechnical Institute, Division of Electrotechnology and Materials Science, M. Sklodowskiej-Curie 55/61 Street, 50-369 Wroclaw, Poland
Email: a.iwan@iel.wroc.pl

large phenyl side group present in DAPP along the polymer chain can reduce the crystallinity and increase the solubility of the polyazomethines.[15]

In order to investigate the influence of phenylphenanthridine moieties on optoelectrical applications of polyazomethines one polyazomethine with phenylphenanthridine sub-units (PAZ-PV-Ph) was synthesized. The structural characterization of the polymer was performed by nuclear magnetic resonance (NMR) and Fourier transform infrared (FTIR) spectroscopy techniques, completed with thermal, optical, electrochemical, theoretical and electrical investigations. As far as the authors are aware, this is the first time that the HOMO-LUMO levels completed by theoretical calculation of the polyazomethine containing vinylene bonds are reported.

Experimental

Materials and methods

All chemicals were purchased from Sigma-Aldrich and used as received. TiO_2 films and powders were obtained as described in Iwan et al.[10] Proton nuclear magnetic resonance (^{1}H-NMR) spectra were recorded on a Bruker AC 300 MHz spectrometer using chloroform ($CDCl_3$) as solvent and tetramethylene sulfone (TMS) as the internal standard. Infrared (IR) spectra were acquired on a 560 MAGNA-IR NICOLET Spectrometer using KBr pellets. UV-vis spectra were recorded as thin films on the quartz substrate and in chloroform solution by using Jasco V670 spectrophotometer. The solutions were spread on quartz glass using the spin-coating method. Quartz substrates were purified using organic solvents such as chloroform and acetone. Characteristic parameters related to speed (880 rpm) and time (10 s) of rotation were applied to spin-coating equipment. All parameters (transmission, reflectivity, and film thickness) which are necessary to calculate the absorption coefficient (α) were measured using JASCO V670 spectrophotometer and its original software. Calculation of layer thickness (d) was made in UV/Vis range from reflectance measurements ($d = 200$ nm). The scattering phenomenon was taken into consideration. Current–voltage characteristics were detected using Keithley 6517B electrometer. Thermogravimetric analyses (TGA) were performed on a Perkin Elmer apparatus at a heating rate of 10° min^{-1} under nitrogen. The surface morphology investigations of the PAZ-PV-Ph were performed in air using a commercial Innova AFM system from Veeco company. Measurements were done in tapping mode and phase imaging. Local contrast data processing was also made. Typical cantilever (about 40 N m^{-1} and < 10 nm tip curvature) was used. Electrochemical measurements were carried out using Eco Chemie Autolab PGSTAT128n potentiostat. Platinum wire (diam. 1 mm), platinum coil and silver wire served as working, auxiliary and reference electrodes, respectively. Potentials were referenced with respect to ferrocene. Thin film of the polymer was cast on the working electrode from solutions in tetrahydrofuran (THF) and dried in air. Differential pulse voltammetry experiments were conducted in a standard one-compartment cell, in acetonitrile (Acros Organics), under argon. 0.1 mol L^{-1} tetrahydrofuran (THF) and Bu_4NPF_6 (Aldrich, 99%) was used as the supporting electrolyte.

Computational details

The conformations of the PAZ-PV-Ph monomers and dimers, built with aromatic ends, and a PEDOT oligomer containing five unit cells as well as the infinite polymer, using periodic boundary conditions, were optimized by the well known hybrid density functional method B3LYP.[16] The medium size 6-31(d) Gaussian basis set was adopted. The computational code GAUSSIAN03[17] was used. Electronic structure analyses were performed based on Kohn-Sham frontier orbitals and corresponding eigenvalues, The acronyms HOMO and LUMO stand for highest occupied molecular orbital and lowest unoccupied molecular orbital, respectively.

Synthesis of PAZ-PV-Ph

2,5-Bis(hexyloxy)-1,4-bis[(2,5-bis(hexyloxy)-4-formylphenylenevinylene]benzene (1 mmol), 3,8-diamino-6-phenylphenanthridine (DAPP) (1 mmol), *p*-toluenesulfonic acid (PTS) (0.004 g) and 10 mL of *N,N*-dimethylacetamide (DMA) were introduced into a 20 mL, two-necked, round-bottomed flask equipped with a magnetic stirrer, a reflux condenser and a nitrogen inlet. The mixture was stirred and heated at 160 °C for 20 h in an oil bath. After cooling the reaction mixture was poured into 50 mL of methanol. Polymer was purified first by washed with methanol (about 300 mL) and acetone (about 150 mL) and later washed in Soxhlet apparatus (hot methanol, 40 h). The polymer was finally dried at 50 °C under reduced pressure. Brown powder, Yield: 70%, ^{1}H-NMR (300 MHz, $CDCl_3$, ppm) $\delta = 8.77$ (s, HC=N–), 8.66, 8.13, 7.92, 7.55–7.62, 7.12, 7.23 (m, H_{ar}), 4.09 (m, –O–CH_2), 3.42 (m, CH_2 side chain), 1.89–1.90 (m, CH_2 side chain), 1.62 (CH_2), 1.27–1.38 (m, CH_2 side chain), 0.85–0.93 (m, CH_3). IR spectrum (KBr pellet, cm^{-1}): 3395, 3382, 2921, 2853, 1679 (HC=O), 1620 (HC=N), 1598, 1530, 1473, 1416, 1375, 1236, 1187, 1011, 968, 856, 805, 698. Anal. calcd for $(C_{79}H_{101}N_3O_6)_n$ (1187.00): C, 79.86; H, 8.51; N, 3.54. Found: C, 76.77; H, 7.12; N, 3.84.

Device fabrication

Current density-voltage measurements were performed on ITO/polymer/Al, ITO/TiO_2/polymer/Al and ITO/PEDOT/

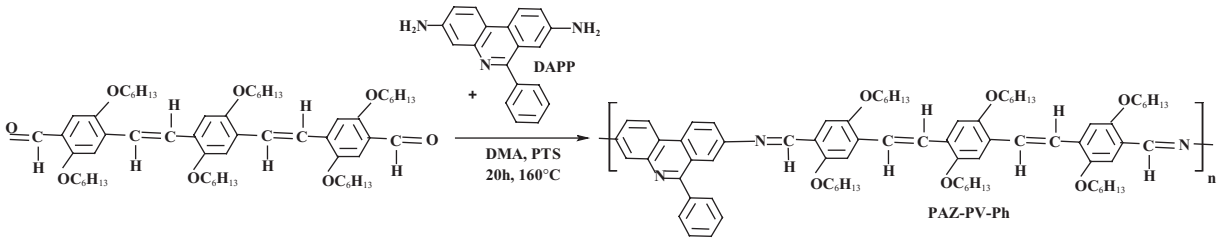

Figure 1. Synthetic route and chemical structure of polyazomethine PAZ-PV-Ph.

polymer:TiO_2/Al devices. The polymer solution (1w/v % in chloroform) was spin-cast onto ITO-covered glass substrate, ITO/TiO_2 or ITO/PEDOT substrate with angular speed 1000 turns min^{-1} by 10 s at room temperature. Residual solvent was removed by heating the film in a vacuum at about 50 °C. The Al electrode (about 0.50 cm^2 area) was prepared on the polymer film surface by vacuum deposition at a pressure of 5×10^{-4} Torr. PEDOT interlayer was spin-coated from water solution.

Table 1. Thermal stability and the surface parameters of polyazomethine PAZ-PV-Ph.

TGA			
$T_{5\%}$ (°C)[a]	$T_{10\%}$ (°C)[a]	$T_{25\%}$ (°C)[a]	Char yield (%)[b]
346	382	434	48
Surface statistics[c]			
R_a (nm)	R_{ms} (nm)	Skew	Kurtosis
1.56	2.84	−3.388	18.317

[a]$T_{5\%}$, $T_{10\%}$, $T_{25\%}$,: temperatures at 5, 10, 25% weight loss, respectively.
[b]Residual weight when heated to 800 °C in nitrogen.
[c]Values calculated for scanning field 5 μm × 5 μm (25 m^2 scan area), surface area ratio: 1.0068

Results and discussion

In the present study polyazomethine containing the vinylene group in the main chain was investigated, namely the fully conjugated polyazomethine, hereafter referred to as PAZ-PV-Ph (see Figure 1). PAZ-PV-Ph was synthesized using a simple one-step condensation procedure in DMA solution. No attempts were made to optimize the polymerization conditions. In the next step of the investigation the authors plan to investigate polyazomethines based on DAPP and such dialdehydes as 2,5-thiophenedicarboxaldehyde and 2,5-bis-(3,7-dimethyloctyloxy)-terephthalaldehyde. Moreover, in the authors previous work the optical properties (UV-vis, photoluminescence) of polyazomethine based on 3,8-diamino-6-phenylphenanthridine and 4,4′-diformyltriphenylamine[18]. Chemical structure of the polyazomethine presented in[18] was confirmed by ^{1}H-NMR (8.60 ppm, –CH=N–), FTIR (1621 cm^{-1}, –CH=N–) and elemental analysis (N: found 12.00, calculated 10.18%).

Macromolecular parameters, spectroscopic and thermal data of the obtained polymer have been described in the Experimental section.

PAZ-PV-Ph was obtained in high yield (70%). The ^{1}H-NMR data concerning the investigated polymer are presented in the Experimental section above. For example, in the proton NMR spectrum of PAZ-PV-Ph the imine protons signal was observed at 8.77 ppm. The signals at about 6.6–8.7 ppm were assigned to the aromatic protons. In the FTIR spectrum of polyazomethine PAZ-PV-Ph characteristic imine peak at 1620 cm^{-1} (–HC=N– stretching deformations) was detected. In addition to the –HC=N stretching band, a band at about 1598 cm^{-1} was distinguished and ascribed to the C=C stretching deformations in the aromatic ring. It can be seen that in the case of the phenanthridine units the presence of the nitrogen atom in the aromatic ring caused the appearance of new bands in the FTIR spectrum due to a change in symmetry of the compound and also a change in the electron charge distribution in the aromatic ring in relation to the phenanthridine moiety.[14] It is reflected in the FTIR spectra as the appearance of the additional absorption band at about 1530 cm^{-1}.

Elemental analyses showed quite good agreement between the calculated and found content of nitrogen (0.3%) in the polymer when the repeated unit structure was taken into calculations. However, a deficiency of carbon and hydrogen content of 3.09 and 1.39%, respectively, was observed and this is probably a result of difficulties in burning the polymer. Similar results have been described for other polyazomethines.[7,19]

Thermal properties

Thermal properties of PAZ-PV-Ph were investigated by differential scanning calorimetry (DSC) and thermogravimetric analysis (TGA) experiments. The glass transition temperature of PAZ-PV-Ph determined by DSC was found to be 141 °C. Taking into consideration the chemical structure of the polyazomethines, it was noted that, consistent with their more rigid chains, PAZ-PV-Ph showed a significantly higher T_g value than PAZ-PV (polymer obtained from 2,5-bis(hexyloxy)-1,4-bis[(2,5-bis(hexyloxy)-4-formyl-phenylenevinylene]benzene and poly(1,4-butanediol)-bis(4-aminobenzoate)).[10] The presence of aliphatic repeat sub-unit in PAZ-PV led to a significant decrease in the T_g

Table 2. UV-vis measurements along with oxidation onset potentials, DPV first peak potentials and HOMO energy of the studied polyazomethine PAZ-PV-Ph.

UV-vis					CV		
λ_{max}* (nm)	λ_{max}** (nm)	$\Delta\lambda_{max}$***	$E_g^{opt.}$ (eV)	$E_g^{(r=2)}$ (eV)	E_{onset} (V)	E_p (V)	E_{HOMO}[a] (eV)
285, 432	295, 440	+8	2.15	1.86	0.17	0.44	−4.97

*in chloroform solution, ** in solid state as thin film, *** shift of imine absorption band in solid state in comparison with solution, "+" indicate red shift.
[a]$E_{HOMO} = -4.80 - E_{onset}$

value ($T_g \sim 14.3$ °C).[10] On the other hand the polymers (polyketaniles) obtained from diketones and 3,8-diamino-6-phenylphenanthridine exhibited higher values of T_g as a result of their more rigid structure (T_g 184–200 °C).[13]

The results of TGA are presented in Table 1. The results of TGA experiments using the polyazomethine showed that the obtained polymer PAZ-PV-Ph had good thermal stability with a 5 wt.% loss temperature of about 356 °C. The residue at 800 °C was around 48%.

Optical properties

The UV-vis spectra of the polyazomethine PAZ-PV-Ph were measured for thin films on quartz substrates and in chloroform solution. Thin films were prepared from chloroform solution of the polymer. The absorption spectral data of the polyazomethine are summarized in Table 2. The UV-vis absorption spectra of the PAZ-PV-Ph recorded in chloroform solution and solid state are shown in Figure 5(a) below.

The optical energy band gap was calculated from absorption spectrum (abbreviation $E_g^{opt.}$) and additionally from the absorption coefficient (α) (abbreviation $E_g^{(r=2)}$). The absorption coefficient was calculated from the reflectivity and transmission using the equation:

$$\alpha = \frac{1}{d}\ln\left(\frac{(1-R)^2}{T}\right) \qquad \text{(b)}$$

where T is the transmission, R is the reflectivity and d is the film thickness.[13,14,20,21] This equation represents the absorption coefficient as a function of reflectivity, transmission and layer thickness. The absorption coefficient plot of the PAZ-PV-Ph thin layers is presented in Figure 2. To delimit the energy band gaps, two equations $E_g = 1240/\lambda$ and $\alpha \cdot E = A(E - E_g)^r$ were applied, where α is the absorption coefficient, A is the parameter independent from photon energy, E is the photon energy, E_g is the energy band gap, r is the index corresponding to band to band transition. The energy band gap of the investigated polymer was calculated for index r equal to 2, which is the indirect band to band transition. A linear approximation of the absorption edge was obtained for PAZ-PV-Ph thin layers on quartz from using equation $(\alpha E)^{1/r} = f(E)$ and is shown in Figure 2(c).

For the investigated polymer band formalism was used because thin layers were made from these organic materials by the spin-coating technique and created on the top of the amorphous thin layer of the substrate. The approach adopted has been used to estimate the band gap of amorphous organic compounds. The value of the parameter $r = 2$ is connected with indirect band to band transition. This means that an electron induced on the higher state absorbs not only photon but also affects the phonon. However, in order to confirm exactly that indirect band to band transitions occur it is necessary to do more sophisticated experiments.

Differences between the values of the energy band gap derived from the absorption spectrum and calculated from absorption coefficient are presented in Table 2. the energy band gap value of PAZ-PV-Ph detected from absorption spectrum ($E_g^{opt.}$) was higher than the value of $E_g^{(r=2)}$ calculated from equation$\alpha \cdot E = A(E - E_g)^r$. Differences between the values of the energy band gaps obtained from the absorption spectrum and calculated from absorption coefficient were small (0.29 eV).

In solution and in solid state the polymer PAZ-PV-Ph exhibited two absorption peaks (see Table 2, Figure 2). In chloroform solution polymer exhibited two absorption bands, the first in the range of 285–340 nm and the second one in the range of 432–450 nm (see Table 2 and Figure 2(a)). In the PAZ-PV-Ph film the first peak around 295 nm was characteristic for absorption of phenylphenantridine, and the peak at about 440 nm corresponded to the absorption of azomethine bond. The maximum of the second absorption band of PAZ-PV-Ph in solid state was about 8 nm red shifted in comparison with the absorption band in solution (Table 2). This behavior suggests the existence of so-called *J*-aggregates, characterized by red-shifted absorption spectra.[22]

Electrochemical measurements

The electrochemical properties of the drop-cast thin film of PAZ-PV-Ph were studied using differential pulse voltammetry, in acetonitrile solution containing 0.1 mol L^{-1} Bu_4NPF_6 (see Table 2 and Figure 3).

PAZ-PV-Ph exhibited irreversible oxidation behavior, due to the well-known instability of electro-oxidation

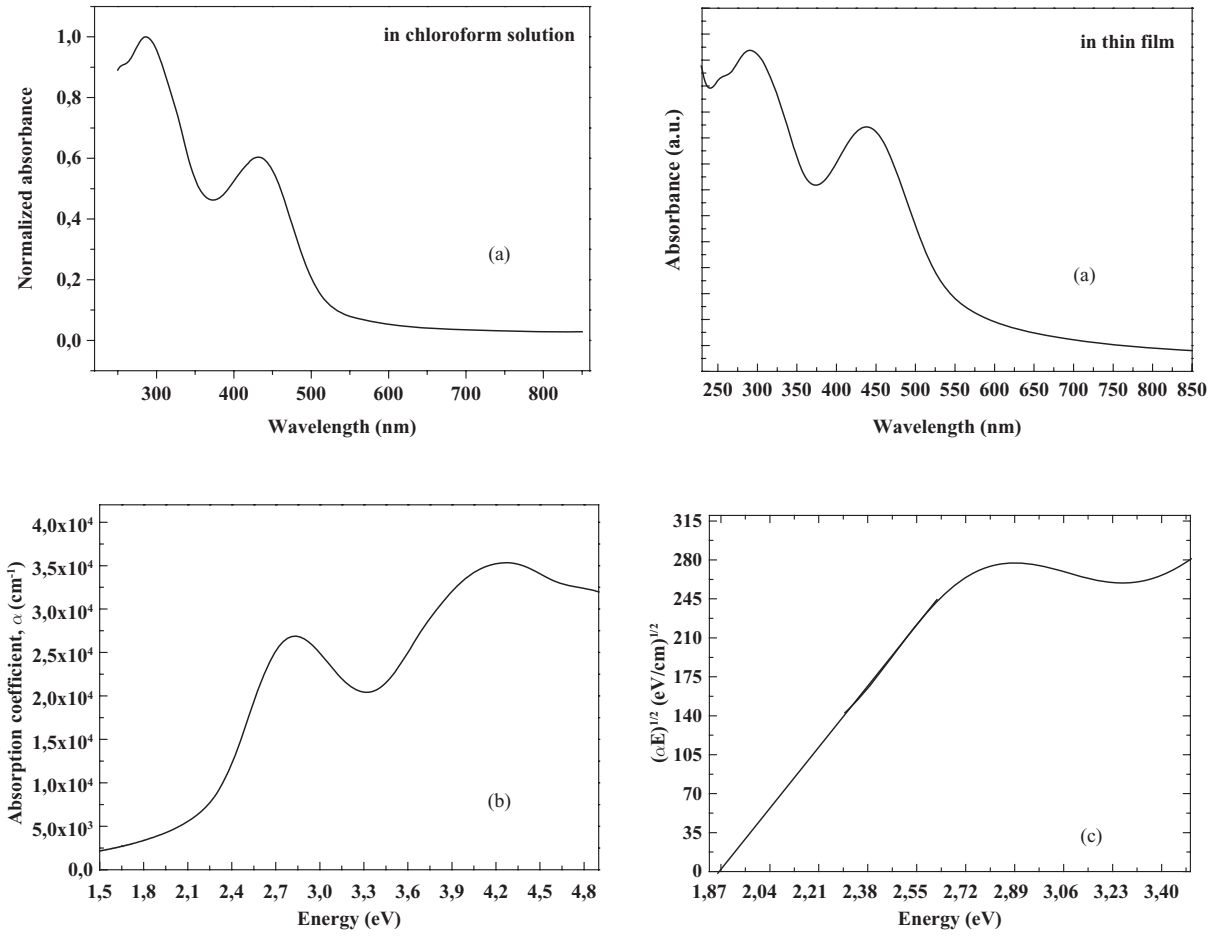

Figure 2. (a) UV-vis normalized absorption spectra of PAZ-PV-Ph in chloroform solution and in film deposited on quartz substrate; (b) absorption coefficient; and (c) linear approximation of absorption edge.

products of arylimines.[23] The oxidation onset of PAZ-PV-Ph was observed at 0.17 and is much lower than typically observed for diarylimines[23] and close to oxidation onset of dialkoxy-substituted PPVs (0.26–0.29 V).[24] Therefore it can be assumed that the first oxidation process occurs on the PPV-like segments, or, possibly on the phenylphenanthridine moiety. HOMO energy (ionization potential) of PAZ-PV-Ph was calculated using the widely-applied equation $E_{HOMO} = -4.80 - E_{onset}$ (Table 2).[25] No reduction processes were detected in the investigated potential range, i.e. down to −1.7 V vs F_c (the reduction of imine linkages)[26] and of the PPV-like segments[24] should appear below −2.0 V), hence the electrochemical E_g of PAZ-PV-Ph was greater than ca. 1.9 eV, in agreement with the values determined from UV-Vis measurements.

The irreversibility of electrochemical oxidation of arylimines in acetonitrile was first described in 1972 by Masui and Ohmori.[23] The oxidation peak is irreversible, regardless of the switching potential. Cyclic voltammograms with the switching potential just above the first oxidation peak were recorded, but no reduction peak on the reverse scan was noted. While it may be true that in strictly anhydrous acetonitrile the oxidation product may be more stable, acetonitrile itself is a nucleophile that may react with the oxidized imine. The acetonitrile used was Sigma-Aldrich HPLC grade (< 0.01% water at time of opening), the

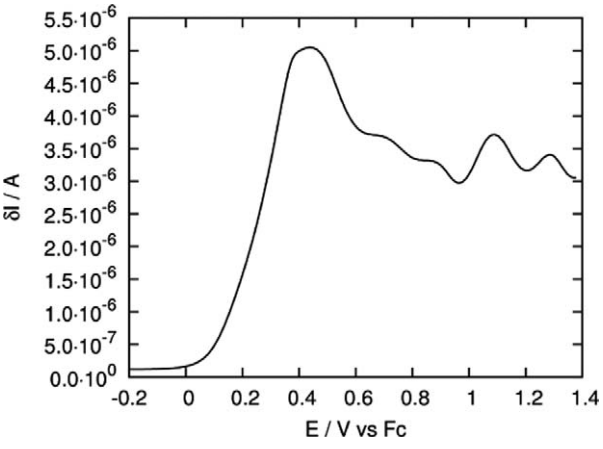

Figure 3. Differential pulse voltammograms of thin films of PAZ-PV-Ph.

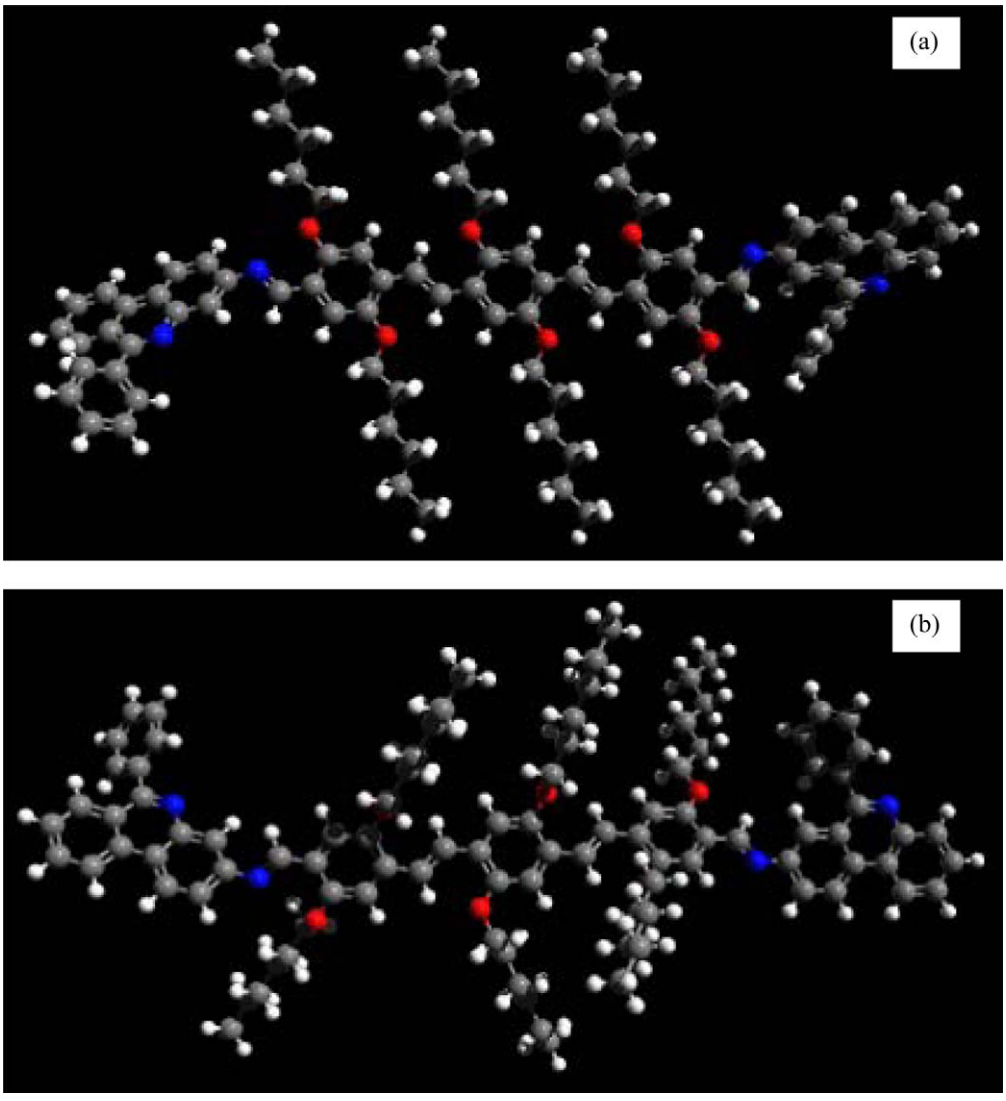

Figure 4. Planar ground state (a) and twisted conformation (b) of PAZ-PV-Ph monomer as obtained from B3LYP/6-31(d) calculations.

electrolyte was dried in vacuum. More anhydrous conditions required (due to quick absorption of moisture from the lab atmosphere, even using ordinary inert gas techniques) operation in a glove box, which was not available to the present authors, who are not aware of any literature precedent of a reversible oxidation of arylimines. As a matter of fact, PF_6^- is less prone to hydrolysis than BF_4^-.[27] Acid-catalyzed hydrolysis of PF_6^- is very slow.[28]

Theoretical calculations

Polymer chain conformations and supramolecular polymer structures in solution and in the solid state are known to play an important role to the opto-electronic properties of conjugated polymers.[29] It is thus desirable to perform a conformational analysis of PAZ-PV-Ph polymer, as well as a comparison of their electronic structures with those of the other components of the devices described below, namely the polymer PEDOT and TiO_2 (anatase).

The alkoxy lateral chains attached to the phenylene vinylene units present in PAZ-PV-Ph are usually optimized, in the gas phase, within the phenyl ring plane. However, considering the low energy involved in the lateral chain rotation, the optimizations were allowed to start from an out-of-plane conformation of the alkoxy chains. These systems have several local energy minima. The out-of-plane twisting of lateral chains induces small torsion angles between neighboring phenylene vinylene units which affect π-conjugation. The polymer PAZ-PV-Ph, where three phenylene vinylene units are linked to another conjugated fragment (phenylphenanthridine), should be more affected by these torsions. One of the twisted PAZ-PV-Ph monomer conformations is displayed in Figure 4, together with the ground state (absolute minimum energy) conformation.

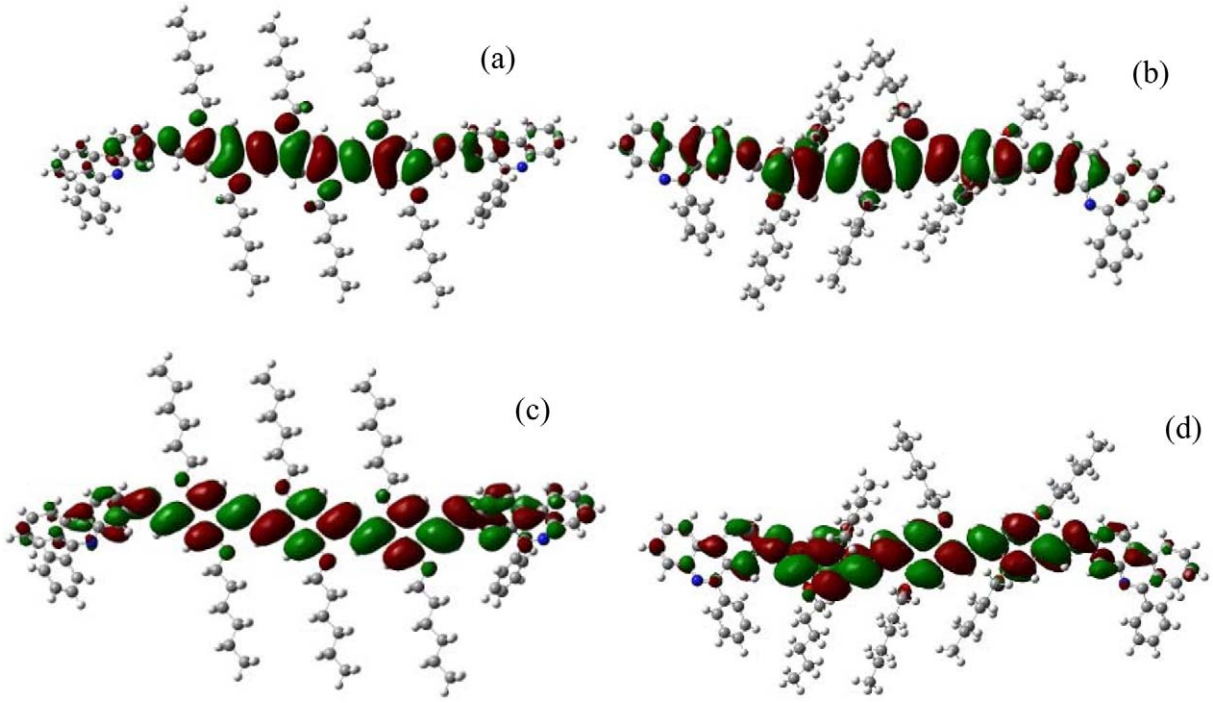

Figure 5. PAZ-PV-Ph HOMO (a, b) and LUMO (c, d) orbitals from B3LYP calculations. (a) and (c) are for the planar monomer; (b) and (d) are for the twisted monomer.

The total energy difference between these structures amounted to 0.34 eV. The effects of small torsion angles on the electronic structure were more important to the HOMO level, which decreased in energy from −4.69 eV in the planar monomer to −5.02 eV. The HOMO-LUMO gap increased as a consequence, from 2.67 eV in the planar monomer to 2.88 eV in its twisted version. The Kohn-Sham orbital isosurface maps are shown in Figure 5. Apparently the twisted conformation decreased the HOMO electronic density in the phenylene vinylene part and extended it to the phenylphenanthridine moiety.

Recent studies on photophysical properties of PPV derivatives[30,31] have demonstrated the important role played by the alkoxy rotations in promoting the above-described small torsion angles between phenylene vinylene units and bending of PPV chains. Moreover, it has been shown that a PPV heptamer presents the same photoluminescence features of the polymer. The unit cell length of PAZ-PV-Ph is of the order of 30 Å, which in comparison with PPV allows two unit cells (dimers) to be adopted as representative of the polymers. It was also preferred to allow the alkoxy rotations so that the HOMO–LUMO gaps obtained from the calculations could be compared with the absorption peak energies in the measurements.

Figure 6 shows the isosurface maps of HOMO and LUMO Kohn-Sham orbitals obtained for PAZ-PV-Ph, together with the respective eigenvalues given in eV. Notice the undulation produced by the alkoxy rotations in the PAZ-PV-Ph polymer backbone, however without affecting conjugation since the orbitals extend through the whole dimer (except for the chain ends, as expected). The calculated HOMO–LUMO gap for PAZ-PV-Ph dimer was 2.80 eV, which agreed with the absorption peak value of 440 nm (2.82 eV) in the solid state. This suggests that the calculated conformation was representative of the chromophores found in the polymer films. Most remarkably, the HOMO energy was in excellent agreement with the experimental estimation for this level (Table 2).

Finally the electronic structure of PEDOT is presented. The optimized conformation of this polymer was calculated to be planar, in agreement with other authors.[32] The comparison between the electronic structures of an oligomer containing five unit cells and the infinite polymer is displayed in Figure 7 in the form of densities of states (DOS). It was noted that the oligomer DOS presented the basic features of the infinite polymer; however the band gap was larger due to the planar backbone. The polymer band gap was calculated to be 1.75 eV.

Current density–voltage experiments (J–U)

Three different types of sample architecture were performed to demonstrate that connecting organic and inorganic compounds improve the electrical properties of devices that can be used as solar cells (SC) or organic light-emitting diodes (OLED). Two devices were fabricated with TiO_2 used as a separate layer or blended with PAZ-PV-Ph (abbreviation PAZ-PV-Ph:TiO_2). Devices

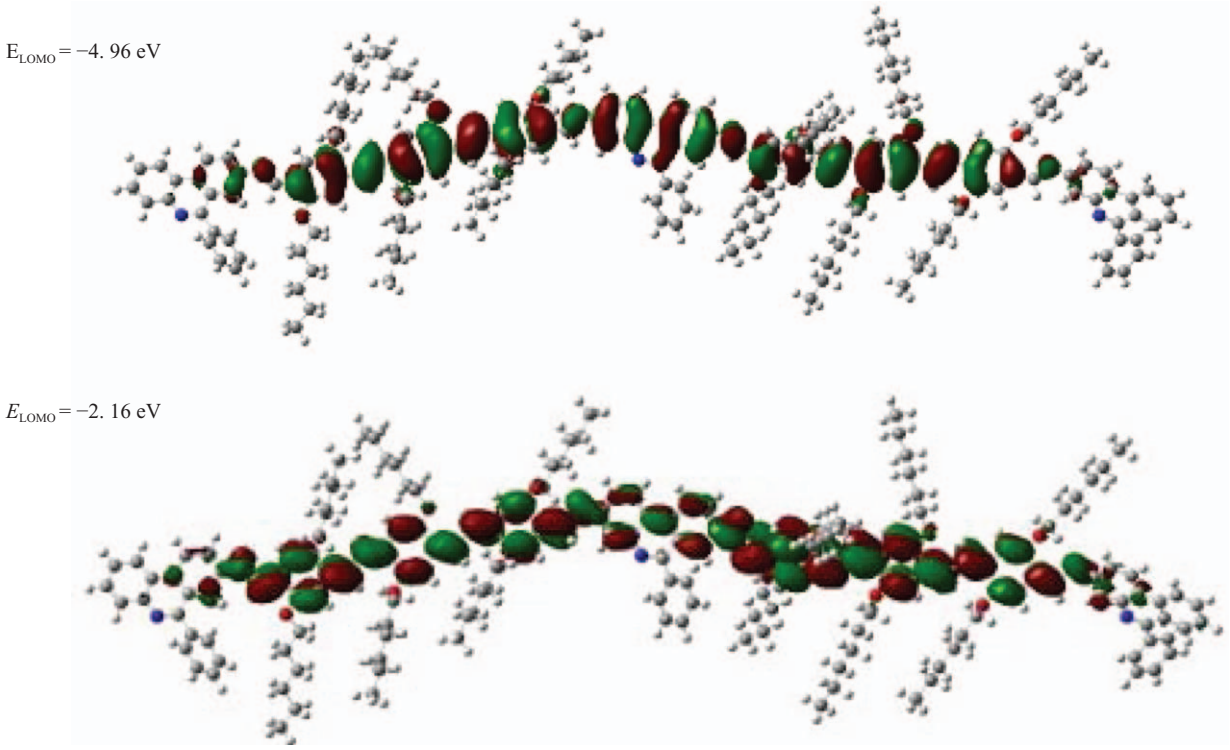

Figure 6. HOMO and LUMO isofurface maps for PAZ-PV-Ph dimers and their eigenvalue energies from B3LYP calculations.

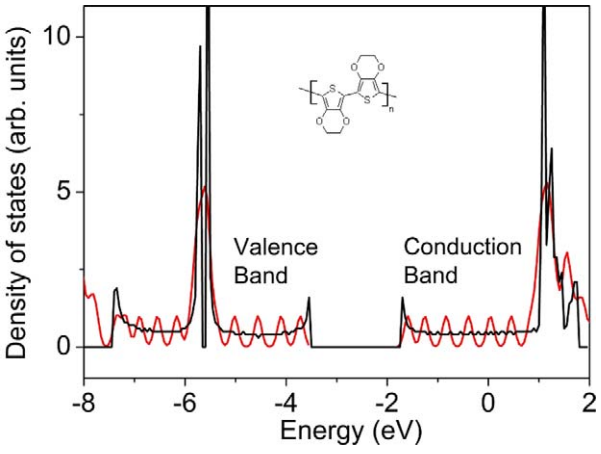

Figure 7. Densities of states of PEDOT (structure shown) obtained from B3LYP calculations: red curves correspond to a finite molecule containing five unit cells and black curves are for the infinite polymer.

having the following architecture: ITO/PAZ-PV-Ph/Al, ITO/TiO_2/PAZ-PV-Ph/Al and ITO/PEDOT/PAZ-PV-Ph:TiO_2/Al in the dark and under light irradiation (halogen lamp, intensity 1000 W m^{-2}) at room temperature were investigated. Indium-tin oxide (ITO)-coated glass was applied as the bottom electrode and was coated with PAZ-PV-Ph, or poly(3,4-ethylenedioxythiophene) (PEDOT) or TiO_2. As the active layer PAZ-PV-Ph or PAZ-PV-Ph blended with TiO_2 was spin-coated. The use of PEDOT as an interlayer caused an increase in the resistance of the device based on PAZ-PV-Ph:TiO_2 active layer. Aluminum was thermally evaporated as a top electrode. The active layer thickness was approximately 200 nm in each device. The samples of nanocrystalline TiO_2 layer and powder were prepared by sol–gel technique.[10] TiO_2 layers were prepared as an anathase phase with a particle size of about 15 nm.[33] For solar cell applications, TiO_2 typically serves as the favored *n*-type semiconductor in the form of an interpenetrating, three-dimensionally continuous percolating matrix with the voids filled with the electrolyte or a *p*-type semiconductor.[34–36] TiO_2 (anatase phase) had a band gap (E_g) of 3.2 eV and absorbs light in the UV region of the solar spectrum.[34–36]

Current density–voltage curves of ITO/PAZ-PV-Ph/Al, ITO/TiO_2/PAZ-PV-Ph/Al and ITO/PEDOT/PAZ-PV-Ph:TiO_2/Al in the dark and during irradiation with light are shown in Figure 8.

First, current density–voltage (J–U) measurements of PAZ-PV-Ph performed on the ITO/PAZ-PV-Ph/Al device in the dark and during irradiation with light (about 5 min of illumination) were investigated. From the obtained results, it was possible to calculate a luminal voltage for illuminated and dark measurements. Differences between device ITO/PAZ-PV-Ph/Al performance in the dark and under irradiation with light were observed. For example, the turn-on voltage of the device ITO/PAZ-PV-Ph/Al was

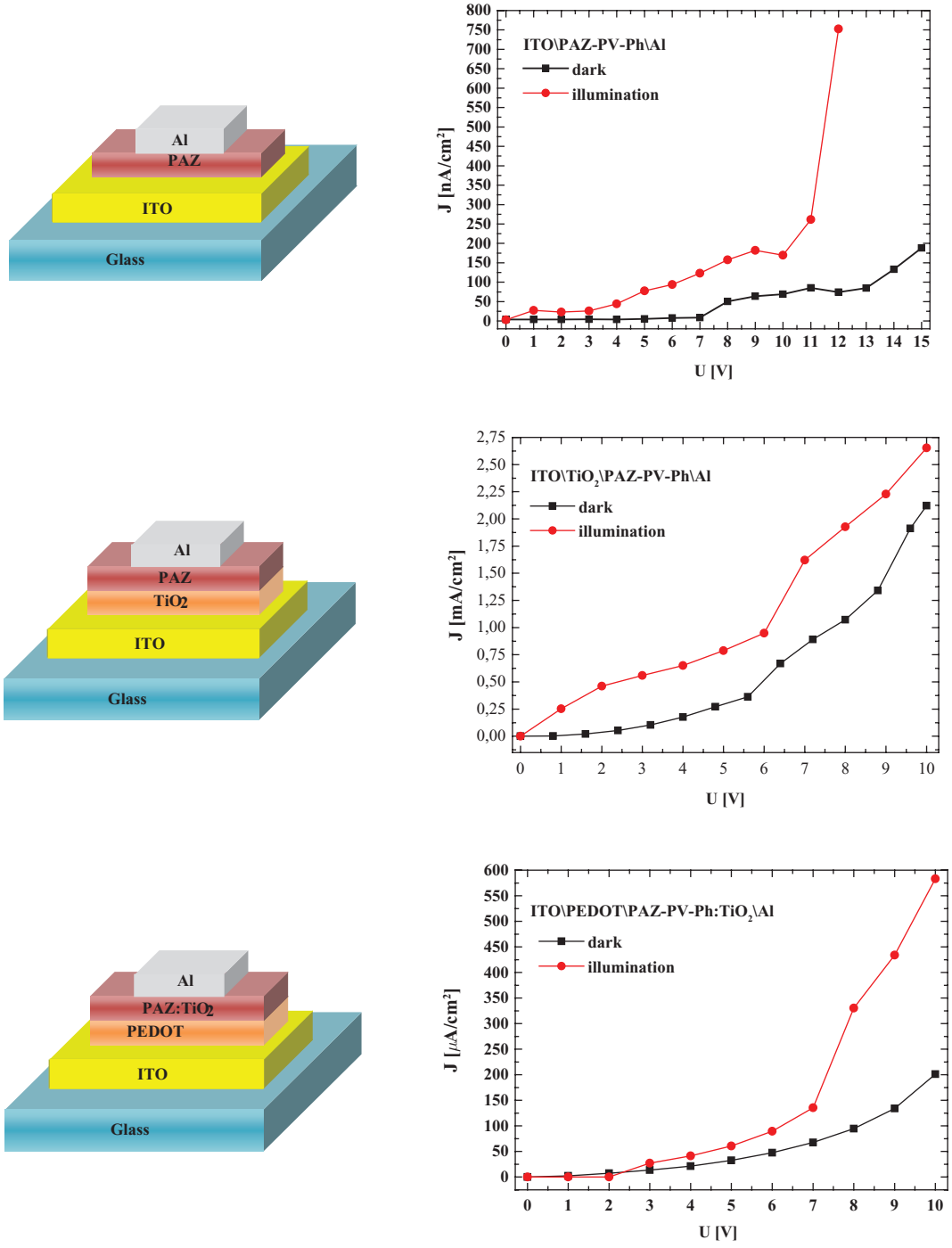

Figure 8. Current density–voltage (J–U) curves of different kind of devices with PAZ-PV-Ph in the dark and during irradiation with light (under illumination 1000 W m^{-2}).

observed at about 4 V under 1000 W m^{-2}, whereas in the dark it was found to be about 7 V (Figure 8). Differences were found along with change of the device structure. For the device ITO/TiO_2/PAZ-PV-Ph/Al the turn-on voltage was observed at about 4 V in room temperature in the dark, while for the same device under illumination it was about 1 V (Figure 8).

Additionally, the influence of PEDOT layer and TiO_2 used as a dopant to PAZ-PV-Ph (PAZ-PV-Ph blended with TiO_2) for current density–voltage characteristic of such a device as ITO/PEDOT/PAZ-PV-Ph:TiO_2/Al was investigated. Differences in the J–U characteristic of devices in the dark and during irradiation with light were observed. For example, for the device ITO/PEDOT/PAZ-PV-Ph:TiO_2/Al

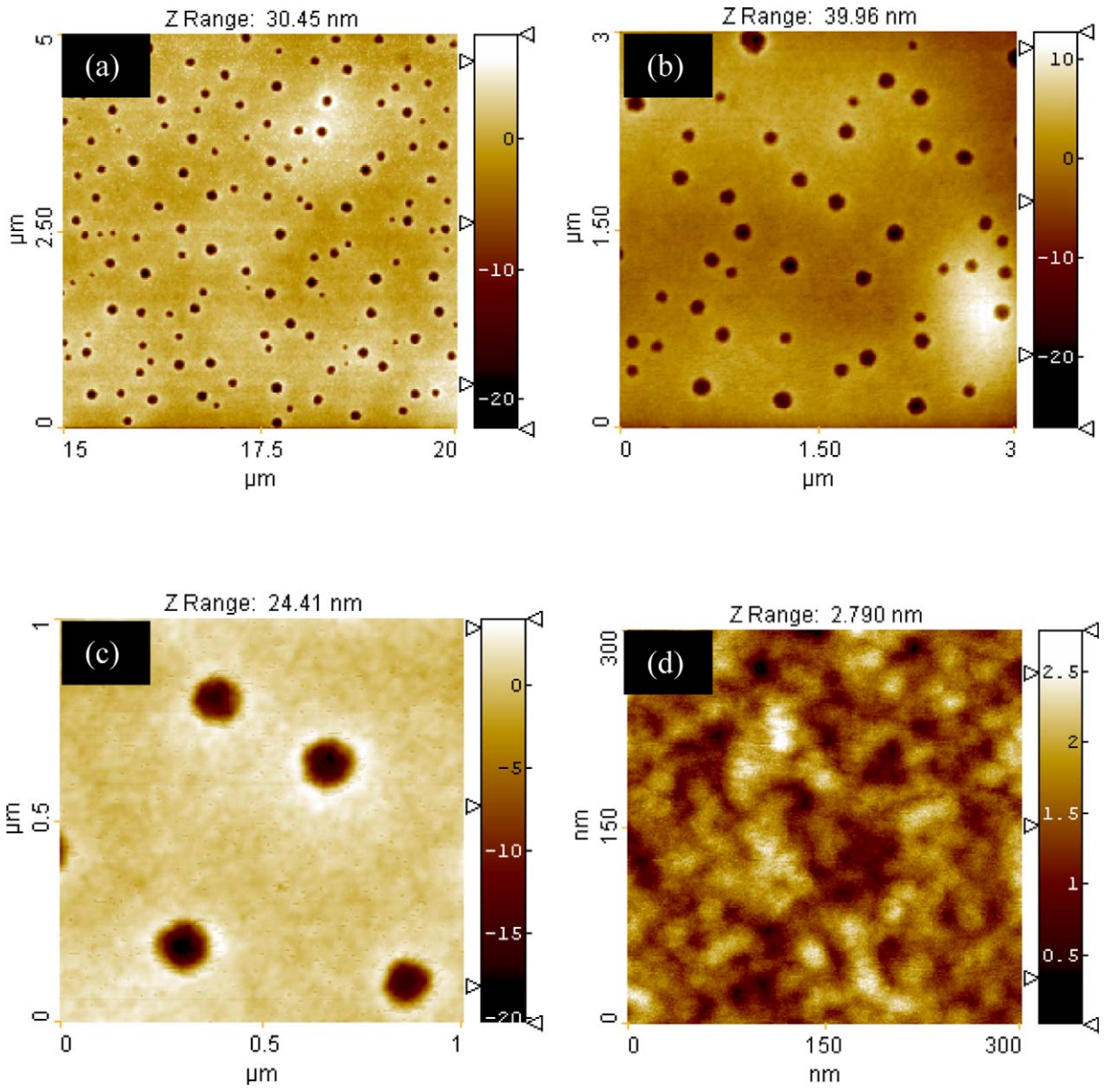

Figure 9. AFM images of the PAZ-PV-Ph: (a) 5 μm × 5 μm (R_{ms} 2.85 nm), (b) 3 μm × 3 μm (R_{ms} 3.71 nm), (c) 1 μm × 1 μm (R_{ms} 2.66 nm) and (d) 300 nm × 300 nm (R_{ms} 0.35 nm).

under illumination the turn-on voltage was observed at about 2 V, whereas for the same device in the dark it was found to be about 3 V (Figure 8).

In the case of devices with PAZ-PV-Ph:TiO_2 active layer, namely PAZ-PV-Ph blended with TiO_2, photogeneration of charges (electrons) was found. This behavior confirmed the influence of the polyazometine structure and the presence of TiO_2 and PEDOT on the J–U characteristic of the polymer. It is evident that for all the devices under illumination, the current rapidly increased with increase of applied voltage.

From the obtained electrical characteristics it was possible to conclude that using TiO_2 material as interlayer between PAZ-PV-Ph and ITO increased the device's current from nA to mA (see Figure 8). In the case of TiO_2 blended with PAZ-PV-Ph as the active layer, an increase of the device's current in comparison with the reference device ITO/PAZ-PV-Ph/Al was observed (see Figure 8).

AFM analysis

In the AFM experiments the influence of the chemical structure of the polyazomethine on the surface morphology of the materials was investigated. Films on the glass substrate were obtained by dissolving the polymer in chloroform at room temperature to form a homogenous solution. Residual solvent was removed by heating the film. No attempt was made to investigate the kind of

solvent on the morphology of polyazomethine. However, it is known that the kind of solvent strongly influences the quality of the film. Figure 9 shows AFM images obtained for PAZ-PV-Ph.

Typical parameters of topography, such as roughness (R_a, R_{ms}) along with skew (the unbalance of height distribution maximum) and kurtosis (the peak's width on height distribution) for the investigated surface are presented in Table 1.

Film of the polyazomethine PAZ-PV-Ph shows a very interesting morphology. Figure 9 presents a typical, planar view of the film topography. The surface of PAZ-PV-Ph reveals homogenously distributed round-shaped holes with the density about 7 per 1 um^2, and dimensions: about 20 nm depth and 50–100 nm diameter. In small area scan (300 nm $\times$ 300 nm) one can see a grainy structure with the typical size of the grain being about 30 nm, and approximately 2.5 nm high. The surface of PAZ-PV-Ph does not contain any ordered forms and is much smoother; however, a significant amount of holes can indicate very high viscosity during the development process. It is very likely that the evaporation of chloroform and reduction of the volume of the material caused opening of air bubbles and, due to high viscosity, these holes were not filled with the material, thus creating the holes that are visible in the presented figures.

Concluding remarks

Polyazomethine with vinylene and phenantridine moieties in the main chain was synthesized by a one-step polycondensation procedure using commercially available monomers. Aromatic polyazomethine PAZ-PV-Ph showed a high glass transition temperature of about 140 °C. PAZ-PV-Ph showed good thermal stability (> 350 °C). In the case of 2,5-bis(hexyloxy)-1,4-bis[(2,5-bis(hexyloxy)-4-formylphenylenevinylene]benzene polymerized with 3,8-diamino-6-phenylphenanthridine (PAZ-PV-Ph) a low band gap (E_g $\sim$ 1.9 eV) was obtained which is promising for opto(electronic) applications. Good electrical properties were observed when TiO_2 was used as an interlayer or blended with PAZ-PV-Ph. Under illumination (1000 W m^{-2}), the ITO/PEDOT/PAZ-PV-Ph:TiO_2/Al device showed the best electrical response. Furthermore, optimization of device architecture may lead to improvements in the electrical and photovoltaic parameters. Electrochemical measurements (DPV) on thin film of the polymer revealed that the oxidation onset was found at 0.17 V. The present results were corroborated by theoretical calculations and showed that PAZ-PV-Ph is a promising material for application in organic devices such as or organic solar cells.

Acknowledgements

The authors thank A. Hreniak for synthesis of TiO_2. M.K. acknowledges the financial support of the Foundation for Polish Science (START scholarship, 2009-2010).

References

1. Iwan A and Sek D. Processible polyazomethines and polyketanils: From aerospace to light emitting diodes and other advanced applications. *Prog Polym Sci* 2008; **33**: 289–345.
2. Niu H, Huang Y, Bai X, et al. Study on crystallization, thermal stability and hole transport properties of conjugated polyazomethine materials containing 4,4'-bisamine-triphenylamine. *Mater Chem Phys* 2004; **86**: 33–37.
3. Niu H-J, Huang Y-D, Bai X-D, et al. Novel poly-Schiff bases containing 4,4'-diamino-triphenylamine as hole transport material for organic electronic device. *Mater Lett* 2004; **58**: 2979–2983.
4. Sek D, Jarzabek B, Grabiec E, et al. A study of thermal, optical and electrical properties of new branched triphenylamine-based polyazomethines. *Synth Met* 2010; **160**: 206–2076.
5. Sek D, Iwan A, Kaczmarczyk B, et al. Supramolecular modification of optical properties of some new polyazomethines. *Mol Cyst Liq Cryst* 2007; **468**: 119–129.
6. Sek D, Iwan A, Jarzabek B, et al. Hole transport triphenylamine-azomethine conjugated system: Synthesis and optical, photoluminescence and electrochemical properties. *Macromolecules* 2008; **41**: 6653–6663.
7. Sek D, Iwan A, Jarzabek B, et al. Characterization and optical properties of oligoazomethines with triphenylamine moieties exhibiting blue, blue-green and green light. *Spectrochim Acta Part A: Mol Biomol Spectrosc* 2009; **72**: 1–10.
8. Liou G-S, Lin H-Y, Hsieh Y-L, et al. Synthesis and characterization of wholly aromatic poly(azomethine)s containing donor–acceptor triphenylamine moieties. *J Polym Sci Part A. Polym Chem* 2007; **45**: 4921–4932.
9. Hindson JC, Ulgut B, Friend RH, et al. All-aromatic liquid crystal triphenylamine-based poly(azomethine)s as hole transport materials for opto-electronic applications. *J Mater Chem* 2010; **20**: 937–944.
10. Iwan A, Palewicz M, Sikora A, et al. Aliphatic-aromatic poly(azomethine)s with ester groups as thermotropic materials for opto(electronic) applications. *Synth Met* 2010; **160**: 1856–1867.
11. Iwan A, Schab-Balcerzak E, Pociecha D, et al. Characterization, liquid crystalline behavior, electrochemical and optoelectrical properties of new poly(azomethine)s and poly(imide) with siloxane linkages. *Opt Mater* 2011; **34**: 61–74.
12. Rohlfing F and Bradley DDC. Non-linear Stark effect in polyazomethine and poly(p-phenylene-vinylene): the interconnection of chemical and electronic structure. *Chem Phys* 1998; **227**: 133–151.
13. Iwan A, Mazurak Z, Kaczmarczyk B, et al. Synthesis and characterization of polyketanils with 3,8-diamino-6-phenylphenanthridine moieties exhibiting light emitting properties. Molecular and supramolecular engineering concept. *Spectrochim Acta Part A: Molec Biomolec Spectr* 2008; **69**: 291–303.

14. Iwan A, Kaczmarczyk B, Jarzabek B, et al. Influence of long-chain aliphatic dopants on the spectroscopic properties of polyketimine containing 3,8-diamino-6-phenylphenanthridine and ethylene linkage in the main chain. Noncovalent interaction: Proton transfer, hydrogen and halogen bonding. *Phys Chem A* 2008; **112**: 7556–7566.
15. Cimecioglut AL and Weiss RA. Aromatic polyamides of 3,8-diamino-6-phenylphenanthridina end their molecular complexes with sulfonated polystyrene ionomers. *Macromolecules* 1995; **28**: 6343–6346.
16. Becke AD. Density-functional thermochemistry. III. The role of exact exchange. *J Chem Phys* 1993; **98**: 5648–5652.
17. Frisch MJ, Trucks GW, Schlegel HB, et al. *Gaussian 03,* Revision E1, Wallingford CT: Gaussian, Inc., 2004.
18. Sek D, Kaczmarczyk B, Jarzabek B, et al. *Nowe fotoluminescencyjne poliazometiny. Modyfikacja polimerow. Stan i perspektywy w roku 2007*. Wroclaw, Poland: Wydział Chemiczny Politechniki Wrocławskiej, 2007, pp. 307–310.
19. Yang CJ and Jenekhe SA. Conjugated aromatic polyimines. 2. Synthesis, structure and properties of new aromatic polyazomethines. *Macromolecules* 1995; **28**: 1180–1196.
20. Rusu GI, Airinei A, Rusu M, et al. On the electronic transport mechanism in thin films of some new poly(azomethine sulfone)s. *Acta Materialia* 2007; **55**: 433–442.
21. Jarzabek B, Weszka J, Burian A, et al. Optical properties of amorphous thin films of the Zn-P system. *Thin Solid Films* 1996; **279**: 204–208.
22. Gierschner J, Cornil J and Egelhaaf H-J. Optical band gaps of p-conjugated organic materials at the polymer limit: Experiment and theory. *Adv Mater* 2007; **19**: 173–191.
23. Masui M and Ohmori H. Anodic oxidation of Schiff bases. Part I. Oxidation of N-benzylidene-p-anisidines in acetonitrile. *J Chem Soc Perkin Trans* 1972; **2**: 1882–1887.
24. Li Y, Cao Y, Gao J, et al. Electrochemical properties of luminescent polymers and polymer light-emitting electrochemical cells. *Synth Met* 1999; **99**: 243–248.
25. Pommerehne J, Vestbeber H, Guss W, et al. Efficient two layer leds on a polymer blend basis. *Adv Mater* 1995; **7**: 551–554.
26. Root DK and Smith WH. Electrochemical behavior of selected imine derivatives, reductive carboxylation, alpha-amino acid synthesis. *J Electrochem Soc* 1982; **129**: 1231–1236.
27. Freire MG, Neves CMSS, Marrucho IM, et al. Hydrolysis of tetrafluoroborate and hexafluorophosphate counter ions in imidazolium-based ionic liquids. *J Phys Chem A* 2010; **114**: 3744–3749.
28. Gebala AE and Jones MM. A rate study of the hydrolysis of the hydroxypentafluoroarsenate(V) anion. *J Inorg Nucl Chem* 1969; **31**: 771–776.
29. Lupton JM. Single-molecule spectroscopy for plastic electronics: materials analysis from the bottom-up. *Adv Mater* 2010; **22**: 1689–1721.
30. Becker K, Da Como E, Feldmann J, et al. How chromophore shape determines the spectroscopy of phenylene–vinylenes: Origin of spectral broadening in the absence of aggregation. *J Phys Chem B Lett* 2008; **112**: 4859–4864.
31. Kemerink M, van Duren JKJ, Jonkheijm P, et al. Relating substitution to single-chain conformation and aggregation in poly(p-phenylene vinylene) films. *Nano Lett* 2003; **3**: 1191–1196.
32. Wijsboom YH, Sheynin Y, Patra A, et al. Tuning of electronic properties and rigidity in PEDOT analogs. *J Mater Chem* 2011; **21**: 1368–1372.
33. Hreniak A, Nyk M, Hreniak D, et al. Optical property, nanocrystalline films, synthesis of europium. *Materials Science-Poland* 2004; **22**: 227–234.
34. Mukherjee B, Karthik C and Ravishankar N. Hybrid sol–gel combustion synthesis of nanoporous anatase. *J Phys Chem C* 2009; **113**: 18204–18211.
35. Nolan TN, Seery MK and Pillai SC. Spectroscopic investigation of the anatase-to-rutile transformation of sol–gel-synthesized TiO2 photocatalysts. *J Phys Chem C* 2009; **113**: 16151–16157.
36. Yan W, Mahurin SM, Overbury SH, et al. Nonhydrolytic layer-by-layer surface sol–gel modification of powdered mesoporous silica materials with TiO_2. *Chem Mater* 2005; **17**: 1923–1925.